Family 18 chitinase–oligosaccharide substrate interaction: subsite preference and anomer selectivity of *Serratia marcescens* chitinase A

Nathan N. ARONSON, Jr*[1], Brian A. HALLORAN*, Mikhail F. ALEXYEV†, Lauren AMABLE*, Jeffry D. MADURA‡, Lakshminarasimhulu PASUPULATI‡, Catherine WORTH§ and Patrick VAN ROEY§

*Department of Biochemistry and Molecular Biology, University of South Alabama, Mobile, AL 36688, U.S.A., †Department of Pharmacology, University of South Alabama, Mobile, AL 36688, U.S.A., ‡Department of Chemistry and Biochemistry, Duquesne University, Pittsburgh, PA 15282, U.S.A., and §Wadsworth Center, New York State Department of Health, Albany, NY 12201-0509, U.S.A.

The sizes and anomers of the products formed during the hydrolysis of chitin oligosaccharides by the Family 18 chitinase A (ChiA) from *Serratia marcescens* were analysed by hydrophilic interaction chromatography using a novel approach in which reactions were performed at 0 °C to stabilize the anomer conformations of the initial products. Crystallographic studies of the enzyme, having the structure of the complex of the ChiA E315L ($Glu^{315} \rightarrow Leu$) mutant with a hexasaccharide, show that the oligosaccharide occupies subsites -4 to $+2$ in the substrate-binding cleft, consistent with the processing of β-chitin by the release of disaccharide at the reducing end. Products of the hydrolysis of hexa- and penta-saccharides by wild-type ChiA, as well as by two mutants of the residues Trp^{275} and Phe^{396} important in binding the substrate at the $+1$ and $+2$ sites, show that the substrates only occupy sites -2 to $+2$ and that additional *N*-acetyl-D-glucosamines extend beyond the substrate-binding cleft at the reducing end. The subsites -3 and -4 are not used in this four-site binding mode. The explanation for these results is found in the high importance of individual binding sites for the processing of short oligosaccharides compared with the cumulative recognition and processive hydrolysis mechanism used to digest natural β-chitin.

Key words: chitin, chitinase, Family 18, glycosidase mechanism, glycosyl hydrolase.

INTRODUCTION

Chitin is a highly stable homopolysaccharide of $\beta(1 \rightarrow 4)$-linked GlcNAc (*N*-acetyl-D-glucosamine). It is the second most prominent biopolymer in Nature next to cellulose, where it is mainly used as a structural matrix in the molecular architecture of arthropodal exoskeleton. Chitinases (EC 3.2.1.14) hydrolyse the $\beta(1 \rightarrow 4)$ linkages of chitin to maintain a balance between the large quantities of carbon and nitrogen potentially trapped in the biomass as insoluble GlcNAc [1]. Biological degradation of chitin is difficult, since its chains are densely packed into microcrystalline substrates through interchain hydrogen-bonding. Adjacent chitin chains can run either parallel (β-chitin) [2] or, commonly, anti-parallel (α-chitin) [3]. In a chitin chain, successive GlcNAcs are rotated 180° relative to each other. Therefore the functional and structural unit is the disaccharide, which by itself is not a substrate for the chitinases.

On the basis of sequence analysis and structural information, the chitinases are classified into two evolutionarily unrelated groups, designated as Families 18 and 19 of the glycosyl hydrolases [4]. Family 18 includes a number of evolved variants: endoglycosidases (such as endoglycosidases H and F), which hydrolyse the chitobiose core of N-linked glycoproteins, and lectins, which are not catalytically active but appear to function when certain tissues undergo differentiation or remodelling. Three-dimensional structures of many Family 18 proteins have been determined by X-ray crystallography [5–22], including several structures of inactive mutants with bound chitin oligosaccharides [7,23,24] as well as with transition-state analogues [12–16,24]. The catalytic domain of Family 18 chitinases consists of a $(\beta/\alpha)_8$-barrel with a deep substrate-binding cleft formed by the loops following the C-termini of the eight parallel β-strands. A glutamic residue at the C-terminus of β-strand 4 has been identified as the proton donor in the hydrolysis reaction [25–28]. This Glu^{315} residue in *Serratia marcescens* chitinase A (ChiA) is asymmetrically placed in the binding cleft that can accommodate at least seven GlcNAc units (Figure 1). The crystal structures of complexes with chitin octa- and hexa-saccharides show that the reducing-end disaccharide of a bound chitin oligosaccharide is the β-anomer and occupies subsites $+1$ and $+2$. GlcNAc at -1 is the glycosyl unit protonated by the catalytic glutamic residue. The disaccharide at $+1$ and $+2$ is thus the leaving group, i.e. the aglycone, and is virtually the exclusive product released from chitin by Family 18 chitinases. Subsites -1 to -5 of the binding cleft can accommodate at least five GlcNAc residues in the glycone region of the substrate. The substrate is hydrolysed between the -1 and $+1$ sites with anomeric retention, so that the released -1 glycosyl sugar remains as β-D-GlcNAc [29]. Double displacement at the glycosyl C-1 is accomplished by a substrate-assisted mechanism in which the carbonyl oxygen of the N-acetyl group at C-2 of the -1 GlcNAc, rather than a protein residue or a water molecule, acts as the nucleophile [25,26,30]. The glycosyl oxygen (O-1) of the -1 GlcNAc becomes protonated by the active-site glutamic residue, and an oxazolinium intermediate is formed as this N-acetyl oxygen reacts at C-1. This positively charged intermediate is stabilized through interaction with a conserved aspartic residue (Asp^{313} in *S. marcescens* ChiA), located two amino acids upstream from the glutamic residue [9–12,31]. The substrate-assisted mechanism is facilitated by an induced conformational change in which the GlcNAc at -1 adopts a skewed-boat conformation, which results in a 90° twist of the linkage with the GlcNAc at $+1$ [25,26].

Abbreviations used: ChiA, chitinase A; FAB, fast atom bombardment; GlcNAc, *N*-acetyl-D-glucosamine; N5, chitopentaose; WT, wild-type.

[1] To whom correspondence should be addressed (e-mail naronson@jaguar1.usouthal.edu).

Atomic co-ordinates of the ChiA E315L mutant have been deposited in the Protein Data Bank under the accession no. 1NH6.

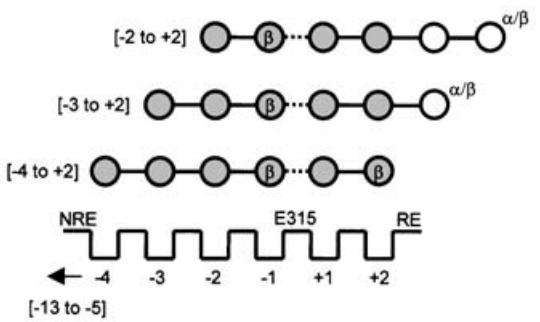

Figure 1 Predicted products from different binding modes of chitin hexasaccharide in the substrate cleft of Family 18 chitinase

All crystal structures of *S. marcescens* ChiA with a bound chitin hexasaccharide show the oligosaccharide at subsites -4 to $+2$, with its reducing-end GlcNAc (RE) at $+2$ as the β-anomer. The catalytic acid/base Glu^{315} (E315) is asymmetrically located in the binding cleft between -1 and $+1$ where hydrolysis occurs ($\cdots\cdots$). The hydrolysis reaction was performed by a substrate-assisted mechanism that retains the configuration of the glycosyl fragment (β-anomer). The shaded circles indicate GlcNAc residues bound in normal subsites. The open circles represent the GlcNAc residues of the aglycone region that do not interact with the protein. Their reducing end is therefore an equilibrium mixture of α/β-anomers. Not shown, but not involved in N6 hydrolysis, are more subsites of the binding cleft (-5 to -13) that can interact with the non-reducing end (NRE) of the glycone region of much longer chitin molecules such as β-chitin. These binding sites are located in both the catalytic and the chitin-binding domains of ChiA.

The disaccharide symmetry of chitin and the multisite nature of the binding cleft of Family 18 chitinases limit the options for various classes and sizes of chitin molecules to align productively in the binding cleft (Figure 1). Crystal structures of complexes of inactive chitinase mutants with oligosaccharides show full occupancy of the binding cleft from subsites -5 (or -4) to $+2$ [7,23,24]. Substrate binding is controlled by a series of aromatic residues. The aglycone disaccharide is inserted edgewise into the cleft and, in ChiA (Figure 2), interacts with three aromatic residues, Tyr^{418} and Phe^{396} at the $+2$ site and Trp^{275} at the $+1$ site. Although Tyr^{418} appears to mark the end of the cleft, it does not interfere with the extension of the reducing end beyond the $+2$ site. Trp^{275} and Phe^{396} form opposite sides of the cleft, stacking against the hydrophobic faces of the GlcNAcs. In contrast, sugars in the glycone component of the substrate lie flat in the cleft and every other GlcNAc in this region has its hydrophobic face aligned with an aromatic amino acid in the cleft floor [-1 (Trp^{539}), -3 (Trp^{167}), -5 (Trp^{170})], whereas the sugars in the even-numbered subsites (-2 and -4) have their hydrophobic surfaces exposed. An important question that is addressed in the present study is the preference of these aromatic subsites used by Family 18 chitinases when hydrolysing oligosaccharide substrates (Figure 1).

A plausible model for the mechanism by which Family 18 glycosidases degrade pure β-chitin has been proposed previously [32–34]. Many Family 18 proteins contain a second domain, namely the chitin-binding domain, which is considered to maintain the enzyme bound to the insoluble substrate so that the reaction can be progressive. The chitin-binding domain of ChiA is located at its N-terminus and has a fibronectin type III fold [5]. The chitin-binding domain contains two tryptophan residues (Trp^{33} and Trp^{69}) which, along with two additional residues (Trp^{232} and Trp^{245}) on the catalytic domain beyond the -5 site of the cleft, appear to be positioned correctly to correspond to binding sites for additional odd-numbered GlcNAcs. Mutagenesis of Trp^{33} and Trp^{69} of the chitin-binding domain of ChiA revealed that they are important for the degradation of crystalline β-chitin, but not for the degradation of oligosaccharides [33]. Likewise, Trp^{232} and Trp^{245} on the catalytic domain of ChiA (Figure 2A) are selective in helping to degrade only the natural polymer [7,33]. Consequently, it appears that the Family 18 chitinases first locate and expose the reducing end of a chitin chain on the surface of the insoluble chitin matrix. In the proposed mechanism, the reducing-end disaccharide at positions $+1$ and $+2$ is then hydrolysed and the enzyme moves symmetrically two GlcNAc residues towards the non-reducing end to degrade the chain processively. New chitin molecules are exposed and hydrolysed by a procession of reducing-end starts from new enzyme molecules that lag behind those which initiated outer-chain degradation. Such a unidirectional hydrolysis of exterior chitin chains explains the sharpening observed at the reducing end of pure β-chitin fibres that have reacted with Family 18 chitinases [32–35].

In the present study, the hydrolysis of soluble chitin oligosaccharides by ChiA is compared with the ordered digestion of natural β-chitin. The sizes and anomeric configurations of the products of hydrolysis of N6 (chitohexaose) and N5 (chitopentaose) are analysed by hydrophilic interaction chromatography [36]. Mutarotation of the products and substrate is minimized by performing the experiments at 0 °C [37]. Analyses are also reported for reactions catalysed by mutants that have an alanine substitution for aromatic amino acids in the substrate cleft, Phe^{396}, Trp^{275} and Trp^{539} (Figure 2). Our results indicate that, when N5 and N6 are substrates for the native chitinase, only four subsites, namely -2 to $+2$, are occupied during hydrolysis and one (for N5) or two (for N6) GlcNAc residues at the reducing end of the substrate are not bound to the enzyme during hydrolysis. These results are in contrast with the results of crystallographic studies of the complexes of inactive mutants with hexa- and octa-saccharides that show all six sites occupied. This unusual enzyme–substrate interaction during chitin oligosaccharide hydrolysis provides important information to explain how Family 18 chitinases can catalyse efficient turnover of chitin in the biosphere.

EXPERIMENTAL

Cloning and site-directed mutagenesis of recombinant *S. marcescens* ChiA

WT (wild-type) ChiA cDNA was isolated from the genomic DNA of *S. marcescens* QMB1466 (A.T.C.C. 990) by PCR amplification. This cDNA was transferred to the multi-cloning site in the expression vector pET23a(+) (Novagen, Madison, WI, U.S.A.), which was used as the template for mutagenesis of all PCRs. Mutagenic primers used in the present study are listed in Table 1. An antisense primer was designed with a two-base change to mutate Glu^{315} to Leu (Table 1). PCR with a forward primer that incorporated the start methionine yielded the approx. 966 bp 5′-half of the ChiA gene. This DNA was digested with *Sal*I and *Sma*I to yield a 423 bp ChiA gene fragment with the single modified codon, E315L ($Glu^{315} \rightarrow$ Leu). After gel purification, it was ligated back into the same unique restriction sites of the normal gene for expression. F396A and W539A mutations were generated using an overlap extension method [38]. The W275A mutation was introduced using a one-tube megaprimer method (A. B. Ekici, O. S. Park, C. Fuchs and B. Rautenstrauss, Technical Tips Online; http://research.bmn.com/). Mutations were verified by double-stranded sequencing at the Iowa State University DNA sequencing facility, and the plasmids were introduced into BL21(DE3) strain (Novagen) for overexpression of WT and mutant proteins.

Protein expression and isolation

All recombinant WT and mutant ChiA cDNAs from *S. marcescens* encoded in-frame C-terminal His_6 tags in the expression vector

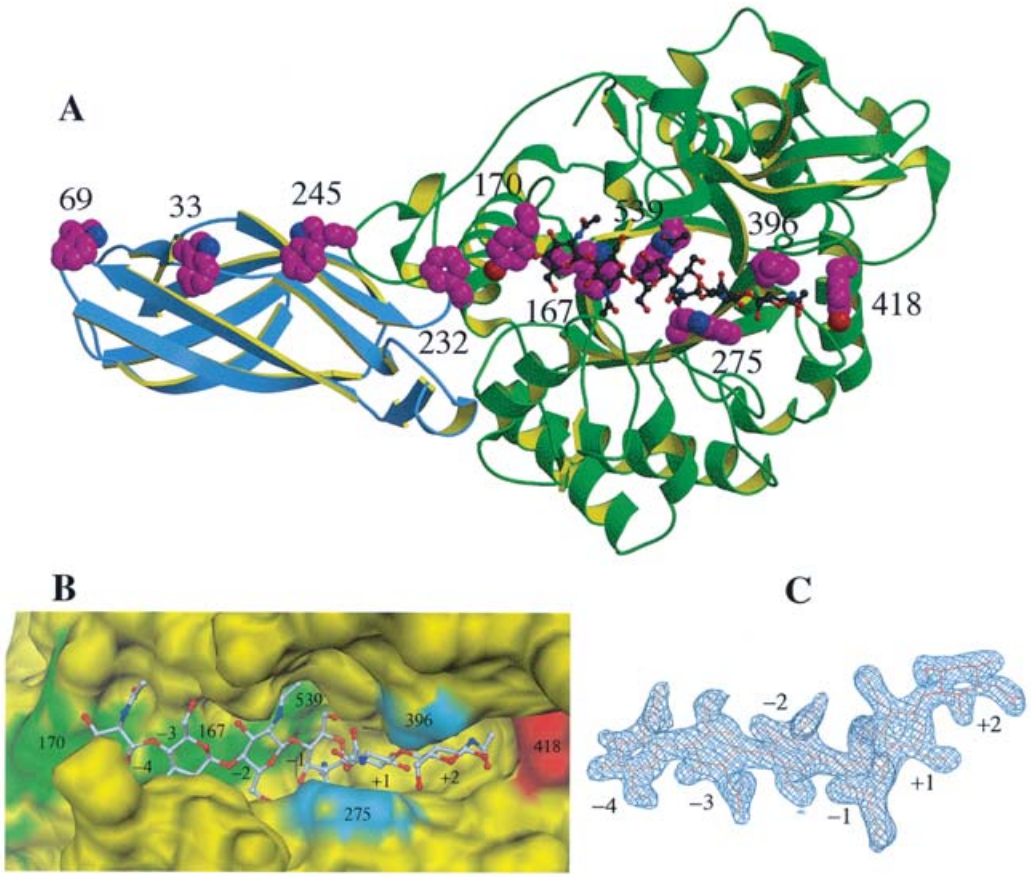

Figure 2 Three-dimensional structure and molecular surface of ChiA (mutant E315L) with the N6 substrate in the binding cleft

(**A**) The N-terminal chitin-binding domain is shown in blue and the C-terminal catalytic domain in green. Aromatic residues that line the substrate-binding cleft are shown in space-filling mode. (**B**) Surface representation of the substrate-binding cleft in ball-and-stick mode. The aromatic residues that interact with the substrate are highlighted. Tyr^{418} (red) interacts with the N-acetyl group of the reducing-end GlcNAc. Phe^{396} and Trp^{275} (cyan) are on opposite sides of the cleft and stack against the hydrophobic faces of GlcNAc sites +2 and +1 respectively. Trp^{539}, Trp^{167} and Tyr^{170} (green) are at the bottom of the cleft and are positioned to interact with the hydrophobic faces of the GlcNAcs at sites −1, −3 and −5 respectively. (**C**) Electron density of the bound N6 substrate as observed in the final $(2F_o - F_c)$-map contoured at the 1.5σ level.

Table 1 Mutagenic primers

Mutated bases are shown in bold/underlined type and restriction sites in bold type. F, forward primer; Rc, reverse-compliment primer.

Name	Sequence
E315L (***SmaI***) (Rc)	CCG**CCCGGG**AAC**AA**CCAGTCG
W275A (Rc)	CGGACAGCGTC**GC**GCCGCCGATC
F396A (F)	GACTTCTATGGCGCT**GC**CGATCTGAAGAAC
F396A (Rc)	GTTCTTCAGATCG**GC**AGCGCCATAGAAGTC
W539A (***SacII***) (F)	CCTGTTCT**CCGCGG**AGATCGACGC
W539A (***SacII***) (Rc)	GCGTCGATCT**CCGCGG**AGAACAGG

pET23a(+) (Novagen), which was used to transform the *Escherichia coli* expression strain BL-21 (DE3) (Novagen) in liquid culture. After calcium chloride transfection, the *E. coli* were grown to exponential growth phase in Luria–Bertani medium (700 ml) with ampicillin (100 μg/ml) at 37 °C and shaking at 200 rev./min. Protein expression in the cells was induced with 1 mM isopropyl β-D-thiogalactoside at 37 °C for 4 h, and the culture was then frozen and kept at −20 °C overnight. After thawing, the cells were pelleted at 5000 ***g*** for 10 min at 4 °C, resuspended in 25 ml of sterile water, and sonicated five times on ice for 30 s using a Branson Sonifer Cell Disruptor 185, equipped with a micro-tip convertor. The sonicated material was centrifuged at 30000 ***g*** for 20 min at 4 °C and the protein in the supernatant (25 ml) was precipitated by adding 9.75 g of $(NH_4)_2SO_4$ with mixing on ice for 1 h. The precipitate was pelleted at 14000 ***g*** for 15 min at 4 °C, resuspended in 15 ml of Ni^{2+}-column binding buffer (5 mM imidazole/0.5 M NaCl/20 mM Tris/HCl, pH 7.9) and centrifuged at 30000 ***g*** for 20 min at 4 °C to remove insoluble materials. The remaining $(NH_4)_2SO_4$ was eliminated by ultrafiltration exchange through a Centripep-10 centrifugal filter device (Millipore, Bedford, MA, U.S.A.) with two 5 ml washes of the Ni^{2+}-column binding buffer. The final non-diffusible material was passed through a 0.45 μm syringe filter and loaded on to a column (1 cm × 4 cm) of HisBind resin (Novagen). The pure His_6-tagged chitinases were eluted from the affinity column according to the manufacturer's instructions (Novagen). The final protein solution was filter-exchanged into 20 mM Tris/HCl (pH 8.0) using a Centripep-10 membrane (Millipore). After sterile filtration, all ChiA preparations were kept at 4 °C. Protein concentration was determined using the Coomassie Plus protein assay reagent kit (Pierce, Rockford, IL, U.S.A.). The purity of protein was determined by SDS/PAGE, which showed each expressed protein to be a single band of the expected molecular mass of 58 kDa. The yield of expressed enzyme was 5–10 mg/l of cultured *E. coli*.

Hydrolysis reactions

Chitin oligosaccharides (di- to hexa-saccharide) were purchased from Associates of Cape Cod (Seikagaku America, Falmouth, MA, U.S.A.). GlcNAc was obtained from Sigma. Reactions were performed in a volume of 20 μl that contained 0.25 mM chitin oligosaccharide and 8.8 mM sodium acetate (pH 5.5), with 20 ng of native ChiA. The reactions for HPLC were performed for 5–15 min at ice temperature to minimize anomerization equilibration of the initial products [37]. For the mutant forms of ChiA, approx. 5–10 times more enzyme was added to produce a hydrolysis rate equivalent to that of WT ChiA. The native enzyme did not exhibit transglycosylation with any oligosaccharide tested under these conditions.

HPLC analysis of reactions

The sizes and anomers of both substrates and products were analysed by HPLC using a Toso-Haas Amide-80 column (4.6 mm × 25 cm; 5 μm particle size) with an Amide-80 guard column (4.6 mm × 1 cm) [36]. A 5 μl sample was injected on to the column, and a Waters/Millipore HPLC system was used to elute chitin fragments isocratically at 1 ml/min with 70 % (v/v) acetonitrile at room temperature (20 °C). Chitin oligosaccharides in the eluate were measured by their UV absorbance at 210 nm and quantified by measuring peak areas using a Waters 740 data module.

MS analysis of the hydrolysis of chitin pentasaccharide ^{18}O-labelled at its reducing end

The procedure of Barr et al. [44] was used to introduce ^{18}O-labelling at the reducing-end GlcNAc of the chitin pentasaccharide. N5 (1.75 mg) was dissolved in 0.175 ml of $H_2{}^{18}O$ (95 % enriched; Icon, Summit, NJ, U.S.A.) and heated under nitrogen at 45 °C for 60 h. The ^{18}O-exchange reaction yielded pure N5 that contained 7.4 times the ^{18}O in the natural pentasaccharide as measured by FAB (fast atom bombardment)-MS. Preparative reactions for both this reducing-end-labelled and natural ^{16}O-chitin pentasaccharide were then performed so that the analyses of the N2 and N3 fragments free of N5 could be accomplished by FAB-MS. For each substrate, the reaction consisted of 0.4 mg of N5 in 0.4 ml of unbuffered $H_2{}^{16}O$, containing 16 μg of native ChiA. After 1 h incubation at 0 °C, a 5 μl sample was assayed by HPLC to confirm complete hydrolysis of N5. The reaction mixture was filtered in the cold using a Centricon-10 membrane (30 min at 4000 ***g***) to remove the enzyme. From the enzyme-free filtrate, a 0.2 ml of sample was dried using a Savant SpeedVac and kept frozen for FAB-MS analysis. Immediately after the dried reaction sample was dissolved in 0.1 ml of water, mass spectra were generated from 2.5 μl using a dithiothreitol matrix (mass of 154). A VG 70-250 SEQ hybrid tandem instrument, equipped with a saddle-field FAB gun and a modified continuous-flow FAB probe, was used for the MS analysis [47]. The fast atom beam was generated from xenon at 6 kV energy and at 1 mA intensity. Positive-ion mass spectra were recorded over the mass range of 50–1200 Da and with a scan rate of 5 s/decade.

Crystallographic studies of the ChiA E315L mutant

The ChiA E315L mutant was prepared as described above for the other ChiA mutants. Protein was concentrated to approx. 4 mg/ml in a buffer containing 10 mM sodium cacodylate (pH 6.5) and 0.5 M NaCl. Crystals were obtained by hanging-drop vapour diffusion methods using a precipitation buffer containing 8–12 % (v/v) ethanol, 0.8–1.3 M NaCl and 0.1 M Hepes (pH 7.0). Complexes with oligosaccharides were prepared by transferring crystals to 50 μl of the precipitation buffer enriched with 10 mM oligosaccharide and 20 % (v/v) glycerol, used as a cryoprotectant, for 24 h. X-ray diffraction data were measured at beamline B9.1 of the Stanford Synchrotron Radiation Laboratory (Menlo Park, CA, U.S.A.) and processed using the program MOSFLM. The crystals belong to space group I222 with cell parameters $a = 78.1$ Å (1 Å = 0.1 nm), $b = 135.2$ Å and $c = 188.1$ Å. The structure was determined by molecular replacement methods, with the program AmoRe [39], using the co-ordinates of the free native ChiA as the model (Protein Data Bank accession no. 1EDQ) and refined using CNS [40]. X-ray diffraction data and refinement statistics are listed in Table 2. Atomic co-ordinates have been deposited in the Protein Data Bank (accession no. 1NH6).

Table 2 Crystallographic data collection and refinement statistics

Values for the highest resolution shell are given in parentheses. R and R_{free} are standard crystallographic factors. $R = \sum(|F_o| - |F_c|)/\sum|F_o|$.

Parameters	Values
Resolution (Å)	36.0–2.05 (2.10–2.05)
I/σ (I)	9.2 (2.4)
R_{sym}	0.069 (0.318)
Completeness (%)	98.6 (87.3)
Redundancy	4.4 (4.0)
R	0.195
R_{free}	0.225
r.m.s. displacement from ideality	
Bond length (Å)	0.0056
Bond angle (deg)	1.25
Dihedral (deg)	25.1
Average thermal parameter (Å^2)	
Protein	24.1
Substrate	21.6
Water	35.8

RESULTS

Crystal structure of the complex of ChiA E315L mutant with N6

The ChiA E315L mutant (Figure 2; Table 2) crystallized into a form that differed from the structures reported previously, including the WT enzyme and the active-site mutants E315Q and D313A [5,23]. The only significant difference between the conformations of the protein molecule in the two crystal forms was a small change in the relative orientations of the catalytic and chitin-binding domains. Superposition of the catalytic domains by least-squares fitting of the α-carbons of residues 135–550 provided an r.m.s. (root-mean-square) displacement of 0.35 Å, but resulted in a displacement of atoms at the end of the chitin-binding domain by approx. 3 Å. This difference was probably caused by differences in crystal packing, but was indicative of flexibility in the linker between the domains, which might be an asset for the functioning of the protein in movement along chains of β-chitin. Crystals of the ChiA E315L mutant were soaked in solutions containing a series of chitin oligosaccharides, from N2 to N6. Interestingly, soaking with N4, and not with any of the other substrates, consistently damaged the crystals. X-ray diffraction data were measured for crystals soaked with N2, N3, N5 and N6, but only those with N5 and N6 yielded interpretable electron density for the oligosaccharide. The N6 substrate bound to subsites -4 to $+2$, in a manner similar to that

observed for the complexes of N6 or N8 with other ChiA mutants [23]. As for the other structures, the −1 GlcNAc was in a twisted-boat conformation (^{1,4}B). In the E315L mutant, Asp^{313} was locked in a position in which it was in hydrogen-bonding contact with Asp^{311} and not with the residue at position 315. This orientation has been suggested previously to correspond to the inactive conformation [23,24], since in this orientation Asp^{313} was incapable of stabilizing the positive charge on the nitrogen of the oxazoline ring of the intermediate. Interestingly, in all complexes of mutant ChiA with intact substrate, Asp^{313} has been found to be in this inactive conformation, whereas in all complexes of native Family 18 enzymes with the transition-state analogue allosamidin, it has been found in the active conformation.

There are now four crystal structures of the complexes of ChiA mutants with hexa- or octa-saccharide (N6 or N8) bound in the substrate cleft (Protein Data Bank accession nos. 1EHN, 1EIB, 1FFR and 1NH6). In each case, subsites −4 (non-reducing end) to +2 (reducing end) were occupied by a GlcNAc. In the two structures with N8 bound, the seventh GlcNAc residue occupied the −5 subsite, whereas the eighth GlcNAc extended somewhat beyond the cleft and remained there against the surface of the catalytic domain. In all four structures, the reducing-end GlcNAc that resided at subsite +2 was in the β-anomer. Binding of the α-anomer at this site leads to an unfavourable interaction with Phe^{396}, which stacks against the carbohydrate ring. Tyr^{418} was located across the substrate-binding cleft at that end, making a hydrophobic contact with the methyl of the GlcNAc at site +2. Modelling experiments (not shown) indicated that Tyr^{418} would not interfere with any reducing-end $\beta(1 \rightarrow 4)$-linked GlcNAc extending beyond the protein surface, suggesting that endo-activity with long oligosaccharide substrates could be possible. On the basis of structural data and the fact that the enzyme functions by retention of configuration, the anticipated products of the processing of a hexasaccharide would be a disaccharide (from subsites +1 and +2) and a tetrasaccharide (from subsites −1 to −4), both as their respective β-anomer (Figure 1). Similarly, processing of a pentasaccharide would be expected to yield a disaccharide and a trisaccharide, both as the β-anomer.

Hydrolysis of chitin hexa- and penta-saccharides by WT ChiA

Analysis of the sizes and anomers of the products of a partial reaction of N6 (Figure 3B) by WT ChiA after 15 min at 0 °C showed two unexpected results: (1) some trisaccharide was formed that was mostly (71 %) in the β-anomer (Table 3), and (2) the N4 product contained more α-anomer (52 %) than β-anomer (48 %). Similar results for the hydrolysis of N6 have been reported for three other Family 18 chitinases [41–43]. On the basis of the asymmetric positioning of the catalytic acid/base Glu^{315} in the substrate cleft, the observed N3 product appeared when some N6 substrate occupied only positions −3 to +2; therefore, the reducing-end GlcNAc of the hexasaccharide had to extend beyond the catalytic domain (Figure 1). A 71 % β-anomer yield for N3 was consistent with half the N3 fragments, the glycone from the −3 to −1 subsites, being 100 % β-anomers owing to the retentive mechanism, and the other half, the aglycone component, being approx. 60/40 α/β-anomers owing to the absence of steric interaction between the reducing end and the enzyme. The tetrasaccharide fragment that was produced from N6 was expected to appear from the non-reducing end, sites −4 to −1, which would yield 100 % β-anomers rather than the 48 % observed (Table 3). To confirm the accuracy of the Amide-80 column in analysing anomers of these earliest products, a sample of the 15 min N6 reaction was separated from the enzyme by centrifuge filtration

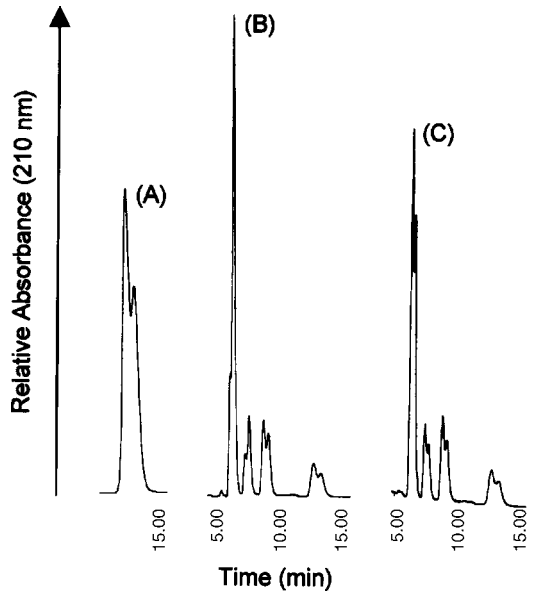

Figure 3 Partial hydrolysis of N6 by native *S. marcescens* ChiA

(**A**) Initial N6 substrate (1.25 nmol) in a 5 μl sample was run on the Amide-80 column. Absorbance of the carbonyl of the N-acetyl groups was measured at 210 nm. The α-anomer was eluted before the β-anomer [36] and their equilibrium ratio was 57:43. (**B**) Hydrolysis of N6 (25 nmol) was performed in 0.02 ml of 8.8 mM sodium acetate (pH 5.5), incubated for 15 min at 0 °C with 0.5 μg of native ChiA. After the enzyme was removed by filtration through a Centricon-10 membrane, products in 5 μl of the filtrate were separated by HPLC. The time order of separation in the 14 min run on the Amide-80 column was N2, N3, N4, N6 (left-to-right) [36]. (**C**) A 5 μl sample of the reaction filtrate shown in (**B**) was allowed to undergo mutarotation overnight at 0 °C to reach anomer equilibrium before the products were separated.

Table 3 Expected and observed products of N5 and N6 hydrolysis by WT and mutant ChiA

Bold-type, main products; italics, unexpected minor product; roman, unprocessed substrate. The values in parentheses give the product expected from binding with the reducing-end GlcNAc at site +2.

		Products (% β-anomer)					
Enzyme	Substrate	N1	N2	N3	N4	N5	N6
WT	N6*		**99** (100)	*71* (100)	**48** (100)		41 (0)
	N5†		**100** (100)	**55** (100)		40 (0)	
F396A	N5‡	*100*	**57** (100)	**100** (100)	*100*	36 (0)	
W275A	N5§	*0*	**100**	**100**	*100*	‖(0)	

* Experimental data from Figure 3(B).
† Experimental data from Figure 5(A).
‡ Experimental data from Figure 5(B).
§ Experimental data from Figure 5(C).
‖ Below detection method.

and allowed to equilibrate for 18 h at 0 °C. All products almost reached the expected 60/40 α/β-anomer ratio (Figure 3C).

Pentasaccharide was hydrolysed to completion with WT ChiA to investigate further the discrepancies seen in the products formed from N6 (Figure 4). Again, unexpected results were obtained, since the trisaccharide fragment was an approx. equilibrium mixture of anomers (45/55 α/β-anomer), and not 100 % β-anomers as should have occurred if N5 had occupied −3 to +2 in the substrate cleft. The small amount of N1 formed and the N2 product were both predominately β-anomers. N1 arose from further hydrolysis of the initial N3 fragments. N3 was cleaved to N1 and N2 and was the smallest substrate for ChiA. It was hydrolysed

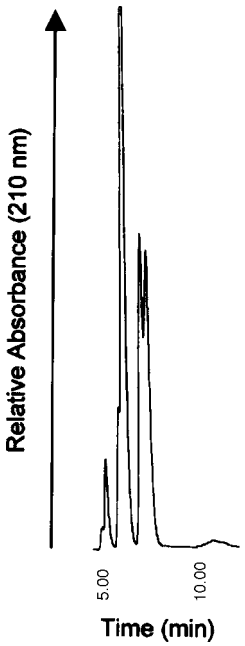

Figure 4 Complete hydrolysis of N5 by native *S. marcescens* ChiA

A preparative sample of N5 (0.4 mg) was digested at 0 °C for 1 h with 16 μg of native ChiA in 0.4 ml of water (unbuffered) as described in the Experimental section. After filtration through a Centricon-10 filter, a 5 μl sample of the reaction was separated by Amide-80 HPLC. The time order of product elution was N1, N2, N3 (left-to-right). Virtually no N5 substrate remained.

much more slowly than the three higher chitin oligomers tested, namely N4, N5 and N6, which were cleaved at nearly equal rates, although increasing according to the oligomer size: N4 < N5 < N6 (results not shown). The observed anomer ratio of the N3 product was only possible if the reducing-end GlcNAc of N5 did not interact with the enzyme, a result consistent with that obtained for N6. This binding mode of the pentasaccharide explains why both α- and β-anomers could be hydrolysed in this complete reaction during a short reaction time, since mutarotation of N5 substrate (and the products) was very slow at 0 °C [37].

A partial reaction of N5 using WT enzyme showed the major products to be N2 and N3 in equal amounts (Figure 5A). The anomeric ratios were similar to those obtained for the complete hydrolysis of N5 (Figure 4): the N2 fragment was comprised of purely β-anomers, whereas N3 was a 45/55 α/β-anomer mixture (Table 3). The remaining N5 substrate was near its equilibrium ratio of 60/40 α/β-anomers.

Confirmation of the four-subsite reaction mode of WT ChiA by MS

Similar to a study by Barr et al. [44] that determined which end of cellulose oligosaccharides was cleaved by five different cellulases, we labelled the reducing end of the chitin pentasaccharide with ^{18}O by an exchange reaction in $H_2{}^{18}O$. In a preparative digestion at 0 °C, there was complete hydrolysis of this ^{18}O-labelled N5 to N3 and N2 (see Figure 4). MS showed that the N3 product had an $^{18}O/^{16}O$ ratio of 2.1, 20-fold greater than the ratio for N3 released from natural N5 (Figures 6B and 6D). The N2 fragment from ^{18}O-labelled N5 had very low ^{18}O content ($^{18}O/^{16}O$ ratio of 0.24; see Figures 6A and 6C). These results showed that virtually all the N3 products came from the reducing end of N5. This confirmed that the four-subsite binding of N5 was the mode of action of the native Family 18 chitinases during the hydrolysis of this size of chitin oligosaccharide. Further proof comes from the fact that WT ChiA hydrolyses both the α- and β-anomers of N5 at equal rates (Figure 7), which can occur only if the reducing-end GlcNAc is not bound by the enzyme.

Hydrolysis of chitin pentasaccharide by the ChiA F396A mutant

The experiments outlined above show that hydrolysis of N5 and N6 by WT ChiA primarily takes place when the substrate occupies

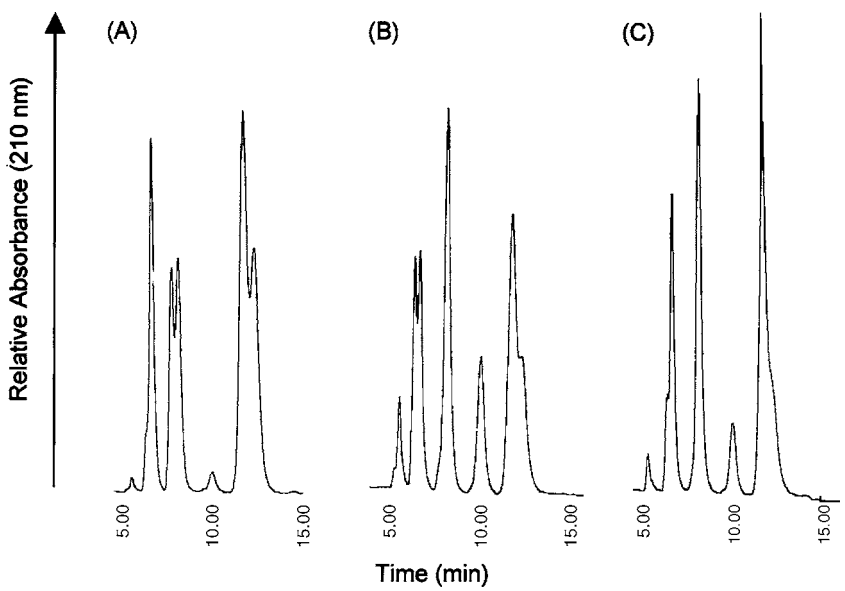

Figure 5 Partial hydrolysis of N5 by native and active-site mutant forms of *S. marcescens* ChiA

All reactions were in a total volume of 0.02 ml, containing 2.5 mM N5, 8.8 mM sodium acetate (pH 5.5) and one of the following enzymes: (**A**) 0.02 μg of native ChiA, (**B**) 0.12 μg of the ChiA F396A (+2 site) mutant and (**C**) 0.12 μg of the ChiA W275A (+1) mutant. After 10 min incubation at 0 °C, a 5 μl sample of each reaction was analysed by HPLC on the Amide-80 column. The order of elution of oligosaccharides and GlcNAc is as described in the legends to Figures 3 and 4.

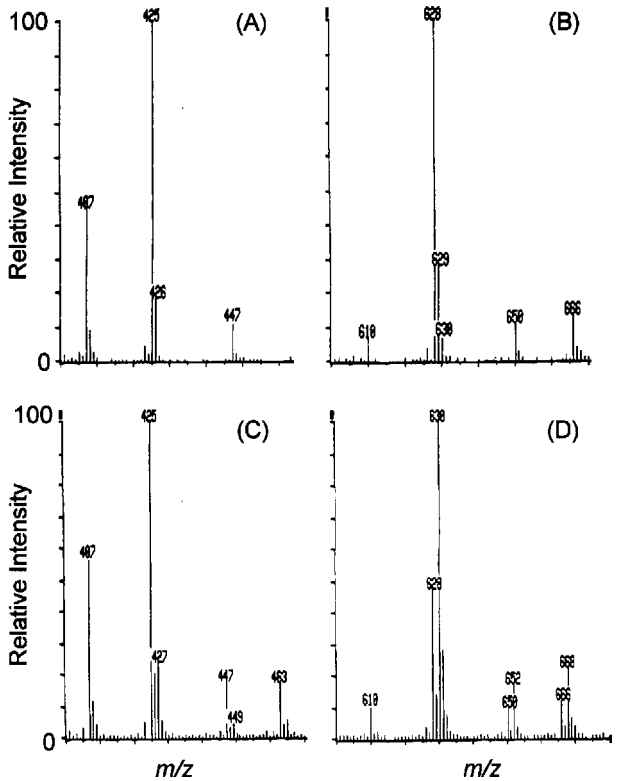

Figure 6 Positive FAB-MS of the reaction products from N5 after complete hydrolysis by native ChiA (see Figure 4)

(**A**, **B**) Natural [^{16}O]N5 substrate; (**C**, **D**) reducing-end-labelled [^{18}O]N5 substrate. (**A**, **C**) Mass range (*m*/*z*) for chitin [^{16}O]disaccharide $H^+/Na^+/K^+$ was 425/447/463; (**B**, **D**) mass range (*m*/*z*) for chitin [^{16}O]trisaccharide $H^+/Na^+/K^+$ was 628/650/666. The ^{18}O-mass fragments were increased by 2 mass units.

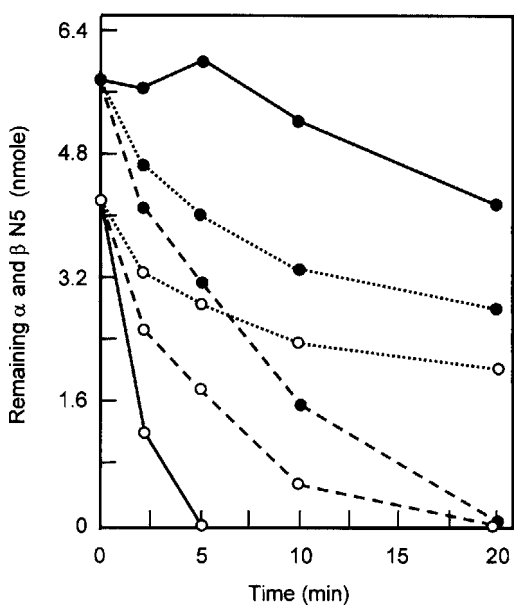

Figure 7 Anomer specificity of *S. marcescens* ChiA and its mutants for N5

Rates of hydrolysis of the α- and β-anomers of N5 at 0 °C were measured by HPLC as described in the Experimental section. ●, αN5; ○, βN5. ·····, WT ChiA; – – –, ChiA F396A (+2) mutant; ——, ChiA W275A (+1) mutant.

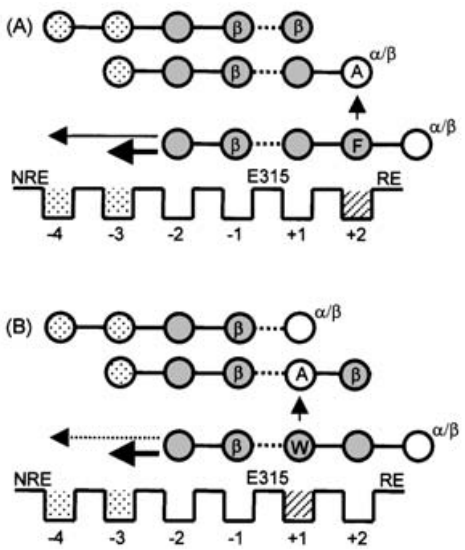

Figure 8 Diagram showing N5 binding in the active-site cleft and products formed by native and mutant forms of ChiA

(**A**) Native ChiA and ChiA F396A (+2) mutant. (**B**) Native ChiA and ChiA W275A (+1) mutant. The enzyme–substrate cleft is depicted as described in the legend to Figure 1. The orientation of N5 (shown fully shaded) in the binding groove of native ChiA is shown closest to the enzyme. Substitution by an alanine residue is shown hatched in the mutated subsites (**A**) F396A (+2) and (**B**) W275A (+1). The two arrows represent the relative amount of N5 that shifts at subsites −3 and −4 (shown stippled) to provide additional binding interactions lost at +2 (**A**) or +1 (**B**) due to alanine substitution.

subsites −2 to +2, with only a small amount of N6 hydrolysis occurring with the substrate at −3 to +2. To investigate further this four-subsite binding mode and the roles of cleft aromatic residues in aligning oligosaccharide substrates, we analysed the products formed during N5 hydrolysis by ChiA mutants at the +1 and +2 subsites (see Figure 2B). The F396A mutant (subsite +2) produced two additional products (Figure 5B): N4, a 100% β-anomer, and N1, which was also predominantly its β-anomer (Table 3). Two other striking changes for the F396A chitinase were that the N3 product was 100% β-anomers, whereas N2 was a 43/57 α/β-anomer mixture. These distributions of anomers were reversed compared with those for hydrolysis of N5 by the WT enzyme (Figure 5A). The remaining N5 slightly favoured its α-anomer over the equilibrium mixture, but the α- and β-anomers were hydrolysed at equivalent rates (Figure 7). This implies that there was no steric selectivity at the reducing end of this substrate by the F396A (+1) mutant. As illustrated in Figure 8(A), the loss of the hydrophobic stacking interaction with the +2 GlcNAc in the F396A mutant appeared to shift the primary binding site of the substrate mostly one, or sometimes two, positions towards the non-reducing end, allowing additional interactions at subsite −3 or at subsites −3 and −4. Subsite −3 contained Trp[167], which would stack hydrophobically with a GlcNAc (Figure 2), and this appears to be the most significant adaptation to the loss of binding at the +2 position. Thus the major initial products formed by F396A chitinase were N3 and N2. N3 was 100% in the β-anomer, owing to binding at the −3 to −1 sites and the retentive nature of the enzyme mechanism, and N2 was in a mixed α/β-anomer ratio, since the absence of Phe[396] decreased the steric selectivity of subsite +2 and allowed hydrolysis of both α- and β-anomers of N5 (Figures 7 and 8A). A smaller amount of the N5 substrate shifted two positions to include the −4 subsite (Figure 8A). In this case, the N4 glycone fragment from subsites −4 to

−1 remained in β-anomer form. All N1 products were also in the β-anomer (Figure 5B), probably owing to steric specificity being maintained at the +1 position by a still normal Trp^{275} (Figure 8A). Although the α- and β-anomers were hydrolysed at approximately the same rate (Figure 7), this selective requirement of N5 β-anomer to form the N4 and N1 products was probably the reason for the remaining N5 to favour slightly the α-anomer (Table 3).

Hydrolysis of chitin pentasaccharide by the ChiA W275A mutant

Trp^{275} was at the +1 site and was important because the aglycone fragment left this position once substrate-assisted hydrolysis of the β(1 → 4) linkage between the +1 and −1 GlcNAc residues occurred. The W275A mutant enzyme remained active and formed products from N5 that were different in both size and anomer conformation from those produced by the WT enzyme (Figures 5A and 5C). The pattern of products was again consistent with the substrate shifting one or two positions towards the non-reducing end, mostly occupying −3 to +2 with some positioned −4 to +1 (Figure 8B). The W275A mutant produced different products when compared with the F396A mutant (Figures 5B and 5C): W275A hydrolysed the β-anomer of the N5 substrate almost exclusively (Figure 7), the N2 product was its β-anomer (Figure 5C and Table 3) and smaller amounts of N4 and N1 were produced, mostly with N1 being its α-anomer. These results are consistent with preferential binding of N5 to the −3 to +2 sites, which allowed the −3 hydrophobic stacking by Trp^{167} to compensate for the loss of similar substrate interactions at the +1 site. Only a small quantity of N5 shifted one subsite further, occupying −4 to +1 (Figure 8B).

DISCUSSION

Degradation of insoluble β-chitin by Family 18 chitinases, including those from *S. marcescens* [33] and *Bacillus circulans* [34], involved progressive removal of reducing-end disaccharides. Consistent with this mechanism, the crystal structures of hexa- and octa-saccharide complexes of inactive mutants of ChiA showed that the substrate bound in the substrate-binding cleft occupying sites −5 (or −4) to +2, where the cleavage site was between the −1 and +1 sites and the reducing-end GlcNAc occupied the +2 site (Figure 2). In contrast, our analysis of the products formed during the hydrolysis of N5 and N6 chitin oligosaccharides by WT ChiA and binding site mutants indicated that these small substrates bound to ChiA at sites −2 to +2 during hydrolysis. In this binding mode, substrates larger than the tetrasaccharide, including N5 and N6, extended beyond the enzyme at their reducing end, and hydrolysed disaccharides were released from the non-reducing end of the oligosaccharides. Depending on the type of chitin substrate, β-chitin or a chitin oligosaccharide, ChiA could remove a disaccharide from either the reducing or non-reducing end. The disaccharide was always the primary product since it was the structural and functional unit of a chitin molecule. The difference as to the disaccharide being the glycone or aglycone component was due to variation in the binding mode for short oligosaccharides compared with native chitin substrates, which was probably a result of differences in their interaction patterns. All evidences indicated that the aromatic residues in the binding cleft were most important in binding and positioning the substrate for effective catalysis. Towards the reducing end, the binding cleft contained three aromatic residues, Tyr^{418}, Phe^{396} and Trp^{275}. The first two interacted with the +2 GlcNAc and the last interacted with the +1 unit. At the non-reducing end, every other subsite (−1, −3, −5, −7 and −9) involved binding to an aromatic residue, Trp^{539}, Trp^{167}, Tyr^{170}, Trp^{232} and Phe^{245} respectively. In addition, Trp^{33} and Trp^{69} on the chitin-binding domain were spaced appropriately to correspond to the −11 and −13 sites. The structure of the chitin matrix dictates that the substrate must enter the cleft from this end and the flexibility of the link between the two domains may play a role in assisting the protein in directing the substrate chain into the cleft at the catalytic domain. The cumulative effects of binding at these multiple sites, with stronger interactions at every other binding subsite, could play a role in the progressive processing of the long substrate, two GlcNAc units at a time.

In contrast with β-chitin, the short N5 and N6 oligosaccharides lacked both the directed binding related to hydrolysis of a long substrate and the ability to interact with many of the binding sites simultaneously. Therefore they interacted initially with the site of the strongest interactions, which occurred symmetrically about the active site, leading to primary occupation of the −2 to +2 sites. The fact that the crystal structures of the complexes of inactive mutants with N6 and N8 substrates are more consistent with binding interactions of natural chitin rather than of the short substrates is probably due to a weaker binding of the substrate to the active-site mutants when compared with the WT protein. In the structures of all complexes of the ChiA mutant with substrate, Asp^{313} was observed in the inactive conformation, rotated away from the residue at position 315 and, most importantly, from the N-acetyl group of the −1 GlcNAc. This was different from the conformation seen in the complexes of Family 18 enzymes with transition-state inhibitors or products [10,12,23,24], where the aspartate residue was found in hydrogen-bonding contact with the nitrogen in the oxazoline ring of the transition-state inhibitor allosamidin or the N-acetyl of the corresponding product GlcNAc. This, together with the absence of the acidic side chain at the catalytic residue, resulted in a decrease in the binding strength at or near the active site. Weaker binding at the active site combined with the absence of hydrolysis of the substrate probably permitted the oligosaccharide to seek the most extended binding interaction. This resulted in binding over the largest possible number of subsites to gain binding energy. There are two recent reports on crystal structures of cartilage glycoprotein-39, a member of the Family 18 lectin group [45,46]. One of the studies [46] suggested that there are two distinct binding affinities along the substrate cleft, with binding of chitin oligomers at −2 to +2 being energetically more favourable than binding to −1 to −4. This variation in affinity for oligosaccharide substrates is now seen to be the case for ChiA, a Family 18 chitinase.

This research was partially supported by the National Institutes of Health (Bethesda, MD, U.S.A.; grant no. GM-59471 to J. D. M. and N. N. A. and grant no. GM-50431 to P. V. R.), United States Public Health Service (Washington, DC, U.S.A.) and National Science Foundation EPSCoR (grant no. 91853 to N. N. A.). The X-ray crystallography facilities of the Stanford Synchrotron Radiation Laboratory are supported by the Department of Energy (Washington, DC, U.S.A.) and the NIH.

REFERENCES

1 Keyhani, N. O. and Roseman, S. (1999) Physiological aspects of chitin catabolism in marine bacteria. Biochim. Biophys. Acta **1473**, 108–122
2 Blackwell, J. (1969) Structure of β-chitin or parallel chain systems of poly-β-(1 → 4)-*N*-acetyl-D-glucosamine. Biopolymers **7**, 281–298
3 Minke, R. and Blackwell, J. (1978) The structure of α-chitin. J. Mol. Biol. **120**, 167–181
4 Henrissat, B. and Davies, G. J. (2000) Glycoside hydrolases and glycosyltransferases. Families, modules, and implications for genomics. Plant Physiol. **124**, 1515–1519
5 Perrakis, A., Tews, I., Dauter, Z., Oppenheim, A. B., Chet, I., Wilson, K. S. and Vorgias, C. E. (1994) Crystal structure of a bacterial chitinase at 2.3 Å resolution. Structure **2**, 1169–1180

6 Hollis, T., Monzingo, A. F., Bortone, K., Ernst, S., Cox, R. and Robertus, J. D. (2000) The X-ray structure of a chitinase from the pathogenic fungus *Coccidioides immitis*. Protein Sci. **9**, 544–551

7 Watanabe, T., Ishibashi, A., Ariga, Y., Hashimoto, M., Nikaidou, N., Sugiyama, J., Matsumoto, T. and Nonaka, T. (2001) Trp122 and Trp134 on the surface of the catalytic domain are essential for crystalline chitin hydrolysis by *Bacillus circulans* chitinase A1. FEBS Lett. **494**, 74–78

8 Fusetti, F., von Moeller, H., Houston, D., Rozeboom, H. J., Dijkstra, B. W., Boot, R. G., Aerts, J. M. and van Aalten, D. M. (2002) Structure of human chitotriosidase. Implications for specific inhibitor design and function of mammalian chitinase-like lectins. J. Biol. Chem. **277**, 25537–25544

9 Terwisscha van Scheltinga, A. C., Armand, S., Kalk, K. H., Isogai, A., Henrissat, B. and Dijkstra, B. W. (1995) Stereochemistry of chitin hydrolysis by a plant chitinase/lysozyme and X-ray structure of a complex with allosamidin: evidence for substrate assisted catalysis. Biochemistry **34**, 15619–15623

10 Waddling, C. A., Plummer, Jr, T. H., Tarentino, A. L. and Van Roey, P. (2000) Structural basis for the substrate specificity of endo-β-*N*-acetylglucosaminidase F_3. Biochemistry **39**, 7878–7885

11 Prag, G., Papanikolau, Y., Tavlas, G., Vorgias, C. E., Petratos, K. and Oppenheim, A. B. (2000) Structures of chitobiase mutants complexed with the substrate di-*N*-acetyl-D-glucosamine: the catalytic role of the conserved acidic pair, aspartate 539 and glutamate 540. J. Mol. Biol. **300**, 611–617

12 Bortone, K., Monzingo, A. F., Ernst, S. and Robertus, J. D. (2002) The structure of an allosamidin complex with the *Coccidioides immitis* chitinase defines a role for a second acid residue in substrate-assisted mechanism. J. Mol. Biol. **320**, 293–302

13 Houston, D. R., Shiomi, K., Arai, N., Omura, S., Peter, M. G., Turberg, A., Synstad, B., Eijsink, V. G. and van Aalten, D. M. (2002) High-resolution structures of a chitinase complexed with natural product cyclopentapeptide inhibitors: mimicry of carbohydrate substrate. Proc. Natl. Acad. Sci. U.S.A. **99**, 9127–9132

14 Houston, D. R., Eggleston, I., Synstad, B., Eijsink, V. G. and van Aalten, D. M. (2002) The cyclic dipeptide CI-4 [cyclo-(L-Arg-D-Pro)] inhibits family 18 chitinases by structural mimicry of a reaction intermediate. Biochem. J. **368**, 23–27

15 Terwisscha van Scheltinga, A. C., Kalk, K. H., Beintema, J. J. and Dijkstra, B. W. (1994) Crystal structures of hevamine, a plant defence protein with chitinase and lysozyme activity, and its complex with an inhibitor. Structure **2**, 1181–1189

16 Matsumoto, T., Nonaka, T., Hashimoto, M., Watanabe, T. and Mitsui, Y. (1999) Three-dimensional structure of the catalytic domain of chitinase A1 from *Bacillus circulans* WL-12 at a very high resolution. Proc. Japan Acad. **75**, 269–274

17 Rao, V., Guan, C. and Van Roey, P. (1995) Crystal structure of endo-β-*N*-acetylglucosaminidase H at 1.9 Å resolution: active-site geometry and substrate recognition. Structure **3**, 449–457

18 Van Roey, P., Rao, V., Plummer, Jr, T. H. and Tarentino, A. L. (1994) Crystal structure of endo-β-*N*-acetylglucosaminidase F_1, an α/β-barrel enzyme adapted for a complex substrate. Biochemistry **33**, 13989–13996

19 Rao, V., Cui, T., Guan, C. and Van Roey, P. (1999) Mutations of endo-β-*N*-acetylglucosaminidase H active site residue Asp-130 and Glu-132: activities and conformations. Protein Sci. **8**, 2338–2346

20 Sun, Y. J., Chang, N. C., Hung, S. I., Chang, A. C., Chou, C. C. and Hsiao, C. D. (2001) The crystal structure of a novel mammalian lectin, Ym1, suggests a saccharide binding site. J. Biol. Chem. **276**, 17507–17514

21 Varela, P. F., Llera, A. S., Mariuzza, R. A. and Tormo, J. (2002) Crystal structure of imaginal disc growth factor-2. A member of a new family of growth-promoting glycoproteins from *Drosophila melanogaster*. J. Biol. Chem. **277**, 13229–13236

22 Mohanty, A. K., Singh, G., Paramasivam, M., Saravanan, K., Jabeen, T., Sharma, S., Yadav, S., Kaur, P., Kumar, P., Srinivasan, A. et al. (2003) Crystal structure of a novel regulatory 40 kDa mammary gland protein (MGP-40) secreted during involution. J. Biol. Chem. **278**, 14451–14460

23 Papanikolau, Y., Prag, G., Tavlas, G., Vorgias, C. E., Oppenheim, A. B. and Petratos, K. (2001) High resolution structural analyses of mutant chitinase A complexes with substrates provide new insight into the mechanism of catalysis. Biochemistry **40**, 11338–11343

24 van Aalten, D. M., Komander, D., Synstad, B., Gaseidnes, S., Peter, M. G. and Eijsink, V. G. (2001) Structural insights into the catalytic mechanism of a family 18 exo-chitinase. Proc. Natl. Acad. Sci. U.S.A. **98**, 8979–8984

25 Brameld, K. A. and Goddard, III, W. A. (1998) Substrate distortion to a boat conformation at subsite −1 is critical in the mechanism of family 18 chitinases. J. Am. Chem. Soc. **120**, 3571–3580

26 Tews, I., van Scheltinga, A. C. T., Perrakis, A., Wilson, K. S. and Dijkstra, B. W. (1997) Substrate-assisted catalysis unifies two families of chitinolytic enzymes. J. Am. Chem. Soc. **119**, 7954–7959

27 Watanabe, T., Kobori, K., Miyashita, K., Fujii, T., Sakai, H., Uchida, M. and Tanaka, H. (1993) Identification of glutamic acid 204 and aspartic acid 200 in chitinase A1 of *Bacillus circulans* WL-12 as essential residues for chitinase activity. J. Biol. Chem. **268**, 18567–18572

28 Kuranda, M. J. and Robbins, P. W. (1991) Chitinase is required for cell separation during growth of *Saccharomyces cerevisiae*. J. Biol. Chem. **266**, 19758–19767

29 Iseli, B., Armand, S., Boller, T., Neuhaus, J. M. and Henrissat, B. (1996) Plant chitinases use two different hydrolytic mechanisms. FEBS Lett. **382**, 186–188

30 Brameld, K. A., Shrader, W. D., Imperiali, B. and Goddard, III, W. A. (1998) Substrate assistance in the mechanism of family 18 chitinases: theoretical studies of potential intermediates and inhibitors. J. Mol. Biol. **280**, 913–923

31 Lu, Y., Zen, K. C., Muthukrishnan, S. and Kramer, K. J. (2002) Site-directed mutagenesis and functional analysis of active site acidic amino acid residues D142, D144 and E146 in *Manduca sexta* (tobacco hornworm) chitinase. Insect Biochem. Mol. Biol. **32**, 1369–1382

32 Sugiyama, J., Boisset, C., Hashimoto, M. and Watanabe, T. (1999) Molecular directionality of β-chitin biosynthesis. J. Mol. Biol. **286**, 247–255

33 Uchiyama, T., Katouno, F., Nikaidou, N., Nonaka, T., Sugiyama, J. and Watanabe, T. (2001) Roles of the exposed aromatic residues in crystalline chitin hydrolysis by chitinase A from *Serratia marcescens* 2170. J. Biol. Chem. **276**, 41343–41349

34 Imai, T., Watanabe, T., Yui, T. and Sugiyama, J. (2002) Directional degradation of β-chitin by chitinase A1 revealed by a novel reducing end labelling technique. FEBS Lett. **510**, 201–205

35 Lindsay, G. J. H. and Gooday, G. W. (1985) Action of chitinase on spines of the diatom *Thalassiosira fluviatilis*. Carbohydr. Polymers **5**, 131–140

36 Koga, D., Yoshioka, T. and Arakane, Y. (1998) HPLC analysis of anomeric formation and cleavage pattern by chitinolytic enzyme. Biosci. Biotechnol. Biochem. **62**, 1643–1646

37 Fukamizo, T. and Hayashi, K. (1982) Separation and mutarotation of anomers of chitooligosaccharides. J. Biochem. (Tokyo) **91**, 619–626

38 Ho, S. N., Hunt, H. D., Horton, R. M., Pullen, J. K. and Pease, L. R. (1989) Site-directed mutagenesis by overlap extension using the polymerase chain reaction. Gene **77**, 51–59

39 Navaza, J. (1994) AmoRe: an automated package for molecular replacement. Acta Crystallogr. A **50**, 157–163

40 Brunger, A. T., Adams, P. D., Clore, G. M., DeLano, W. L., Gros, P., Grosse-Kunstleve, R. W., Jiang, J. S., Kuszewski, J., Nilges, M., Pannu, N. S. et al. (1998) Crystallography & NMR system: a new software suite for macromolecular structure determination. Acta Crystallogr. D **54**, 905–921

41 Koga, D., Sasaki, Y., Uchiumi, Y., Hirai, N., Arakane, Y. and Nagamatsu, Y. (1997) Purification and characterization of *Bombyx mori* chitinases. Insect Biochem. Mol. Biol. **27**, 757–767

42 Fukamizo, T., Sasaki, C., Schelp, E., Bortone, K. and Robertus, J. D. (2001) Kinetic properties of chitinase-1 from the fungal pathogen *Coccidioides immitis*. Biochemistry **40**, 2448–2454

43 Sasaki, C., Yokoyama, A., Itoh, Y., Hashimoto, M., Watanabe, T. and Fukamizo, T. (2002) Comparative study of the reaction mechanism of family 18 chitinases from plants and microbes. J. Biochem. (Tokyo) **131**, 557–564

44 Barr, B. K., Hsieh, Y. L., Ganem, B. and Wilson, D. B. (1996) Identification of two functionally different classes of exocellulases. Biochemistry **35**, 586–592

45 Houston, D. R., Recklies, A. D., Krupp, J. C. and Van Aalten, D. M. (2003) Structure and ligand-induced conformational change of the 39 kDa glycoprotein from human articular chondrocytes. J. Biol. Chem. **278**, 30206–30212

46 Fusetti, F., Pijning, T., Kalk, K. H., Bos, E., Dijkstra, B. W. (2003) Crystal structure and carbohydrate binding properties of the human cartilage glycoprotein-39. J. Biol. Chem., 10.1074/jbc.M303137200

47 Shartava, A., Monteiro, C. A., Bencsath, F. A., Schneider, K., Chait, B. T., Gussio, R., Casoria-Scott, L. A., Shah, A. K., Heuerman, C. A. and Goodman, S. R. (1995) Posttranslational modification of β-actin contributes to the slow dissociation of the spectrin–protein 4.1–actin complex of irreversibly sickled cells. J. Cell Biol. **128**, 805–818

Received 18 February 2003/7 August 2003; accepted 22 August 2003
Published as BJ Immediate Publication 22 August 2003, DOI 10.1042/BJ20030273